DEVELOPMENT OF A POST-DRYOUT HEAT TRANSFER MODEL

Y.J. Wang[a] and C. Pan[a,b,c*]
[a]Institute of Nuclear Engineering and Science, [b]Department of Engineering and System Science, [c]Low Carbon Energy Research Center
National Tsing Hua University, Hsinchu, Taiwan, 30013, R.O.C.
dauw8017@gmail.com; cpan@ess.nthu.edu.tw

ABSTRACT

A one-dimensional mechanistic model for fully-developed post-dryout region is developed in the present work. This model is composed of four conservation equations, i.e. droplet momentum, droplet mass, vapor mass, vapor energy, and a set of closure relations accounting for various heat transfer mechanisms. In particular, a new correlation for the interfacial heat transfer between the vapor and liquid droplets is developed considering the Eckert number effect.

The model provides the detail information including the droplet velocity, droplet radius, heat transfer rate and vapor temperature depicting the mechanism in the post-dryout region. Comparison of the wall temperature predicted with the experimental data in the literature shows that the present model predicts the temperature rise and the degree of thermal non-equilibrium successfully. Over 90% of 319 wall temperature data with the range of P= 30~140 bar, $q"$ = 204~1837 kW/m^2 and G= 380~5180 kg/m^{2}s can be predicted within $\pm 20\%$ with the present model.

KEYWORDS
Post-dryout, liquid deficient film boiling, dispersed flow

1. INTRODUCTION

Beyond the dryout point in a boiling tube with high vapor quality, liquid no longer covers the tube wall and heat is primarily transferred to vapor accompanying with dispersed droplets. This may cause a thermal non-equilibrium phenomenon in which the vapor temperature exceeds saturation temperature and become superheated while the dispersed droplets still remain saturated. In this region, which is called the post-dryout region or liquid deficient region, the heat transfer rate is deteriorated and it will lead to a sudden rise of wall temperature which might damage the wall. Therefore, post-dryout heat transfer is of crucial importance for the safety of a nuclear power plant, or the design of a heat exchanger, etc.

Numerous prediction methods have been proposed in the literature. Empirical correlations are the simplest and the most straightforward methods that use the experimental data to fit the expressions of heat transfer coefficient [1, 2]. This method has strong dependence on the data they used and is limited to the range of experimental data. Phenomenological models consider the thermal non-equilibrium phenomenon with empirical vapor generation rate to calculate the vapor superheat [3-5]. However, the validity of the empirical vapor generation rate is still limited in certain cases.

*Corresponding author

Another predicting method, mechanistic models, give the detail structure and physical properties of the flow. Mechanistic models were first proposed by the several reports published at Massachusetts Institute of Technology in 1960s, and the most quoted model was proposed by Forslund & Rohsenow[6]. Their models were based on the use of conservation equations to describe the heat exchange between wall, vapor and droplets, and consider the effect of heat transfer from wall to contacting droplets. Iloeje et al.[7] extended their research and gave a sophisticated description on droplet-wall interaction. Other researchers followed up with detailed analysis on this mechanism [8-10]. With the presence of dispersed droplets, the study from Varone and Rohsenow[11] proposed a model accounting for the influence of droplets, several studies focus on the hydrodynamic of droplets[12-14] and give a close look of droplet behavior. The mechanistic models presented in the literature cover different degree of complexity ranging from one-dimensional to multi-dimensional analysis and different degree of simplification on various heat transfer mechanisms.

The objective of this paper is to develop a one-dimensional mechanistic model for post-dryout heat transfer, with a wide range of flow conditions. Each heat transfer paths are considered with closure laws studied to modify, if needed, the one in the literature. With the conservation equations and specific heat transfer mechanism description, the thermal non-equilibrium phenomenon is fairly well depicted as well as the wall temperature. More studies are undergoing.

2. MODEL DESCRIPTION

The present model is composed of four basic conservation equations, i.e. vapor mass, vapor energy, droplet mass, droplet momentum, and a set of closure laws. Several assumptions are made to simplify the calculation:

(1) The pressure remains constant.
(2) The temperature of droplets remains at saturation temperature.
(3) Before the onset of dryout, vapor and liquid are in thermal equilibrium.
(4) The droplet diameter is uniform across the tube.
(5) No droplet coalescence occurs.

2.1. Conservation Equations

Momentum balance of liquid droplets

The droplets dispersed in the post-dryout region are accelerated by the buoyancy force and the drag force from the vapor.

$$\rho_l u_d \frac{du_d}{dz} = -g(\rho_l - \rho_v) + \frac{3}{8r_d} C_D \rho_v (u_v - u_d)^2 \quad (1)$$

Where C_D is the drag coefficient, which will be discussed in section 2.3

Mass balance of droplet

The average droplet size is reduced by evaporation due to the effect of vapor convection to droplet (q_{vd}), droplet-wall interaction (q_{wd}), and radiation heat transfer from wall to droplet (q_{rwd}) and from vapor to droplet (q_{rvd}):

$$\frac{dr_d}{dz} = \frac{1}{u_d}\frac{dr_d}{dt} = \frac{-(q_{vd} + q_{wd} + q_{rwd} + q_{rvd})}{u_d(4\pi r^2)\rho_l i_{lv}} \tag{2}$$

q_{vd} , q_{wd} , q_{rvd} , q_{rwd} are to be discussed in section 2.2.

Mass balance of vapor

The decrease in droplet mass contributes to the increase in vapor quality. Thus,

$$G\frac{dx_a}{dz} = -N\rho_l 4\pi {r_d}^2 \frac{dr_d}{dz} \tag{3}$$

Where N is the droplet flux,

$$N = \frac{G(1-x)}{\frac{4}{3}\pi {r_d}^3 \rho_l} \tag{4}$$

Energy balance of vapor

The heat diffused from the wall may be transferred to the liquid droplets through direct contact or radiation, and to the vapor, through forced convection or radiation, to increase the vapor temperature as well as the actual quality. Thus,

$$q''\pi D = q_{wd}''\pi D + q_{rwd}''\pi D + G\frac{\pi D^2}{4}\left[i_{lv} + Cp_v(T_v - T_{sat})\right]\frac{dx_a}{dz} + G\frac{\pi D^2}{4}Cp_v\frac{dT_v}{dz} \tag{5}$$

Rearrangement of above equation leads to the following equation for vapor temperature:

$$\frac{dT_v}{dz} = \frac{4\left(q'' - q_{wd}'' - q_{rwd}''\right)}{GDCp_v} - \left[i_{lv} + Cp_v(T_v - T_{sat})\right]\frac{dx_a}{dz} \tag{6}$$

2.2. Models For Various Heat Transfer Mechanisms

The present model considers all seven heat transfer paths[12]: wall to vapor convection, wall and droplets interaction, vapor to droplets convection, evaporation of droplets, wall to vapor radiation, wall to droplets radiation and vapor to droplets radiation.

2.1.1. Wall to vapor convection

The heat flux from the wall is transferred to vapor and droplets. The contact area ratio between vapor and the wall may be approximated by void fraction. Hence, the relation between heat flux and the wall temperature can be expressed as

$$q'' = q_{wd}''+q_{rwd}''+q_{rwv}''+\alpha h_{wv}\left(T_w - T_v\right) \tag{7}$$

Consequently, the wall temperature can be calculated by the following equation:

$$T_w = T_v + \frac{q''-q_{wd}''-q_{rwd}''-q_{rwv}''}{\alpha h_{wv}} \tag{8}$$

Where q'' is the total heat flux from the wall, q_{wd}'' is the heat flux between wall and droplets due to droplet-wall contact, q_{rwd}'' and q_{rwv}'' are the heat flux transferred by radiation to the droplets and vapor, respectively. The following temperature dependent correlation from Heineman [15] is used in the present work for the heat transfer coefficient between wall and vapor.

$$\begin{aligned} h_{wv} &= \frac{k_v}{D}0.0157\left(\frac{Gx_aD}{\mu_v}\right)^{0.84}\left(\frac{Cp_v\mu_v}{k_v}\right)^{1/3}\left(\frac{L}{D}\right)^{-0.04} \quad for\ \ 6<\left(\frac{L}{D}\right)<60 \\ h_{wv} &= \frac{k_v}{D}0.0133\left(\frac{Gx_aD}{\mu_v}\right)^{0.84}\left(\frac{Cp_v\mu_v}{k_v}\right)^{1/3}\left(\frac{L}{D}\right)^{-0.04} \quad for\ \left(\frac{L}{D}\right)>60 \end{aligned} \tag{9}$$

Where L is the distance from dryout point.

2.1.2. Wall and droplet interaction

The heat transferred from the wall to droplets can be evaluated using Guo and Mishima's model [10]. They assumed that, as a droplet hits the wall, a vapor base is generated at the interface and heat is transferred by film boiling mechanism and obtained the following time-averaged heat flow rate to a single drop:

$$q_{sd} = \pi k_v(T_w - T_{sat})t_R {r_d}^2\left[\frac{32\rho_l\rho_v\Delta h_v u_{dr}}{9\mu_v k_v(T_w - T_s)t_R 2r_d}\right]^{1/4} \tag{10}$$

Where t_R is the droplet residence time, which is defined as the duration time that a single droplet has direct contact with the wall, and can be evaluated using the equation given in [10]. The average droplet-wall contact heat flux can then be calculated as:

$$q_{wd}'' = q_{sd}\frac{\dot{m}_D}{\rho_l\frac{4}{3}\pi {r_d}^3} \tag{11}$$

Where the droplet deposition rate onto a heated wall, $\dot{m}_D$, can be evaluated by the following equation[10]

$$\dot{m}_D = \left[\frac{\mu_l}{D} 0.22 \,\mathrm{Re}_l^{\,0.74} \left(\frac{\mu_v}{\mu_l} \right)^{0.26} \right] (1-\alpha)\rho_l \tag{12}$$

2.1.3. Vapor to droplet convection

It is found in the present study that the convection heat transfer between vapor and droplets is the key mechanism in post-dryout region, which depicts the degree of thermal non-equilibrium and dominate the accuracy of prediction. The heat transfer rate from vapor to droplets per unit length tube is:

$$q_{vd}'' = h_i (T_v - T_{sat}) \tag{13}$$

Where h_i is the interfacial heat transfer coefficient.

Lee and Ryley[16] proposed a model predicting h_i of droplets in high temperature steam. Ban and Kim[17] modified the Lee-Ryley model to account for the effect of thermal non-equilibrium:

$$h_i = \frac{k_v}{d} (2 + 0.74 \,\mathrm{Re}_d^{\,0.5} \,\mathrm{Pr}_f^{\,1/3}) \frac{i_{lv}}{i_v - i_l} \tag{14}$$

Where Re_d is the droplet Reynolds number based on droplet diameter, relative velocity between vapor and droplet, vapor density and mixture viscosity:

$$\mathrm{Re}_d = \frac{\rho_v (u_v - u_d) 2 r_d}{\mu_m} \tag{15}$$

Where the mixture viscosity is to be presented and discussed in section 2.3.

However, the calculation results in the present study shows that the slope of vapor and wall temperature rise is too small, which indicates that the interfacial heat transfer rate needs to be modified. Applying the dimensional analysis, the Nusselt number can be expressed in the form of [18]

$$Nu = fn\left(\mathrm{Re}, \mathrm{Pr}, Ec\right) \tag{16}$$

Where Re, Pr are Reynolds number and Prandtl number, respectively. Ec is the Eckert number, which accounts for the relation between kinetic energy and enthalpy, defined as:

$$Ec = \frac{(u_v - u_d)^2}{Cp_v (T_v - T_{sat})} \tag{17}$$

In this study, the Ban and Kim correlation[17] is modified in the following way

$$h_i = \frac{k_v}{2 r_d} (2 + 0.74 \,\mathrm{Re}_d^{\,0.5} \,\mathrm{Pr}_f^{\,1/3} \, Ec^n) \frac{i_{lv}}{i_v - i_l} \tag{18}$$

The effect of Ec on wall temperature is presented in Figure 1, which shows the strong effect of the exponent of Ec on the trend of temperature rise. The results implicate that the size of the droplets are extremely small, so it is necessary to consider the frictional effect on heat transfer. The viscous dissipation from droplet to vapor at the interface reduces the total heat transfer rate from vapor to droplets. Neglecting this phenomenon will lead to an overestimation of interfacial heat transfer rate. The value of n selected for predicting best-fitted wall temperature is 0.4. This value is used for all the cases of this study.

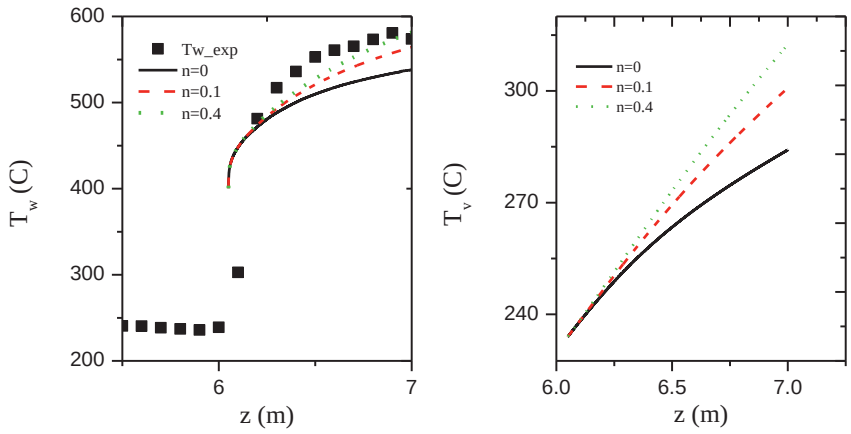

Figure 1. (a) Comparison of predicted wall temperature based on different exponent (b) Comparison of predicted vapor temperature based on different exponent

2.1.4. Radiation heat transfer

The radiation heat transfer among the wall, vapor and droplets in this paper is based on that proposed by Sun et al.[19] with the wall emissivity of 0.4 for Nimonic alloy at high temperature.

2.3. Other Closure Relations

Mixture viscosity

The interactions among the droplets on the mixture viscosity should be considered. The present study adopts the model proposed by Ishii and Zuber [20] for the mixture viscosity and,

$$\mu_m = \mu_l \left(\frac{1-\alpha_d}{\alpha_{dm}}\right)^{-2.5\alpha_{dm}(\mu_l+0.4\mu_v)/(\mu_l+\mu_v)} \tag{19}$$

Where α_{dm} is the maximum packing void fraction, $\alpha_{dm} = 0.62 \sim 1$ for dispersed flow. For the present study, $\alpha_{dm} = 1$ is used.

Drag coefficient

The size of droplets will decrease gradually while they flows downstream, and the change in droplet size and velocity will affect the drag force applied on each droplet. The drag coefficient from Ishii and Zuber[20] is employed in the present work.

$$C_D = \frac{24}{\mathrm{Re}_d}, \quad \text{for } \mathrm{Re}_d < 1 \text{ (Stokes regime)} \tag{20a}$$

$$C_D = \frac{24(1 + 0.1\mathrm{Re}_d^{0.75})}{\mathrm{Re}_d}, \quad \text{for } \mathrm{Re}_d > 1 \text{ (viscous regime)} \tag{20b}$$

Droplet break-up

The diameter of a moving spherical droplet is governed by the Weber number [21] , We, which is a dimensionless number describing the relation between the inertia force and the surface tension:

$$We = \frac{\rho_v (u_v - u_d)^2 2r_d}{\sigma} \tag{21}$$

According to Varone and Rohsenow[11], the critical Weber number in post-dryout region is 17.5. Beyond this value, the surface tension is no longer able to sustain the shape of a droplet and the droplet will breaks up due to the high value of inertia force. The present study adopts the Varone and Rohsenow's droplet break-up criteria for the modeling of droplet size and number density. If break-up occurs,

$$r_d = \frac{1}{2} \frac{We_{cr}\sigma}{\rho_v (u_v - u_d)^2} \tag{22}$$

The droplet number density should be recalculated from above droplet size.

2.4. Dryout Condition

In order to solve for the four differential conservation equations, we need several boundary conditions for numerical integration.

Void fraction

It is found that the accuracy of void fraction at the dryout location is important. The void fraction directly affects the initial droplet velocity, u_d, and hence affects the droplet behavior in the channel. For example, under the condition of high heat flux and low mass flux with high dryout quality (>0.9), different predicting correlation leads to different results in void fraction and the calculated droplet velocities at dryout location, as shown in Table I. Although the difference among the three selected correlations is within 5%, the calculated $u_{d,DO}$ demonstrates large discrepancy. This leads to significantly different wall and vapor temperature distribution downstream, as shown in Figure 2. Although the temperature is slightly under-prediction when the correlation proposed by Ahmad [22] is used, the trend of the temperature rise is more reasonable, and this correlation is adopted in the present study since it predicts the trend of temperature rise well.

$$s = \frac{u_v}{u_d} = \left(\frac{\rho_l}{\rho_v}\right)^{0.205} \left(\frac{GD}{\mu_l}\right)^{-0.016} \tag{23}$$

Table I Comparison of Calculated Void Fraction and Droplet Velocity at the Dryout Point (Case 294of Becker et al[23])

	Void fraction at dryout point with $x_{DO}=0.345$	$u_{d,DO}=\frac{G(1-x_{DO})}{\rho_l(1-\alpha)}$	$We=\frac{\rho_v(u_v-u_d)^2 2r_d}{\sigma}$
Ahmad[22]	0.949	18.6	10.0
Woldesemayat and Ghajar[24]	0.923	12.7	25. (>17.5)
Cioncolin and Thome[25]	0.916	11.2	28.8 (>17.5)

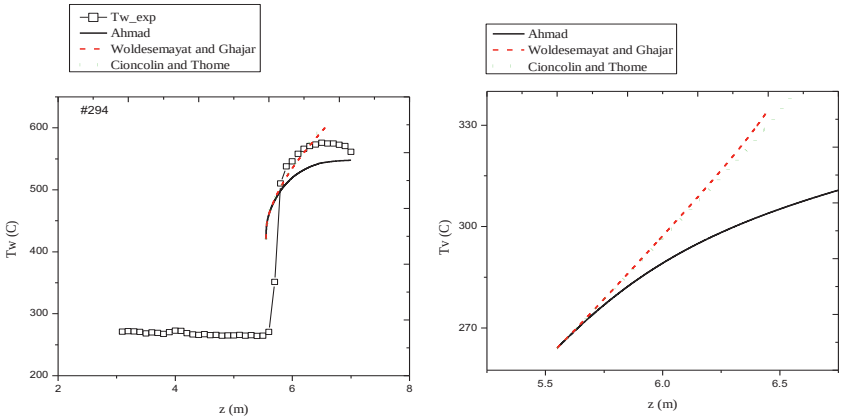

Figure 2. (a) Wall temperature from different void fraction at dryout point (b) Vapor temperature from different void fraction at dryout point (Case 294 of Becker et al.[23])

Droplet size at dryout point

The droplet diameter is one of the key parameter for post-dryout predictions which governs the droplet number density and hence affects the total heat transfer rate. After comparing the calculation from several droplet models ,the model of Kataoka et al.[26] is employed in the coupling computation with above model description:

$$r_d=\frac{1}{2}7.96\times10^{-3}\frac{\sigma\rho_v}{(xG)^2}\left(\frac{\rho_v u_v D}{\mu_v}\right)^{2/3}\left(\frac{\rho_v}{\rho_l}\right)^{-1/3}\left(\frac{\mu_v}{\mu_l}\right)^{2/3} \quad (24)$$

3. SOLUTION METHOD

The differential equations are solved using Runge-Kutta 4 integration technique to obtain the distributions of droplet size, droplet velocity, vapor temperature, vapor quality and wall temperature along the channel. The four differential in section 2.1 with boundary conditions in section 2.4 are solved with step size ≥

5000. 319 data from Bennett et al. [27] and Becker et al. [23] were compared and discussed in the next section.

4. RESULTS AND DISCUSSION

The following results compare the difference between high and low degree of thermal non-equilibrium. Low mass flux will more likely to cause high degree of thermal non-equilibrium. As shown in Figure 3(a), for the case of high degree of thermal non-equilibrium, the vapor temperature and wall temperature will rise continuously along the tube; however, for the case of low degree of thermal non-equilibrium, vapor temperature remains nearly at saturation temperature and the wall temperature reaches an asymptotic value shortly after the dryout location. In the aspect of relative velocity, as shown in Figure 3(b), the relative velocity between vapor and droplet reaches equilibrium in a short distance beyond the dryout location for both cases. However, for the case of high degree of thermal non-equilibrium, the velocity difference between vapor and droplet is higher than the opposite case, which give rise to the existence of dynamic non-equilibrium. The radius of droplets are much smaller for the case of low dryout quality, and the overall heat transfer area are much more larger than that for the case of high dryout quality case.

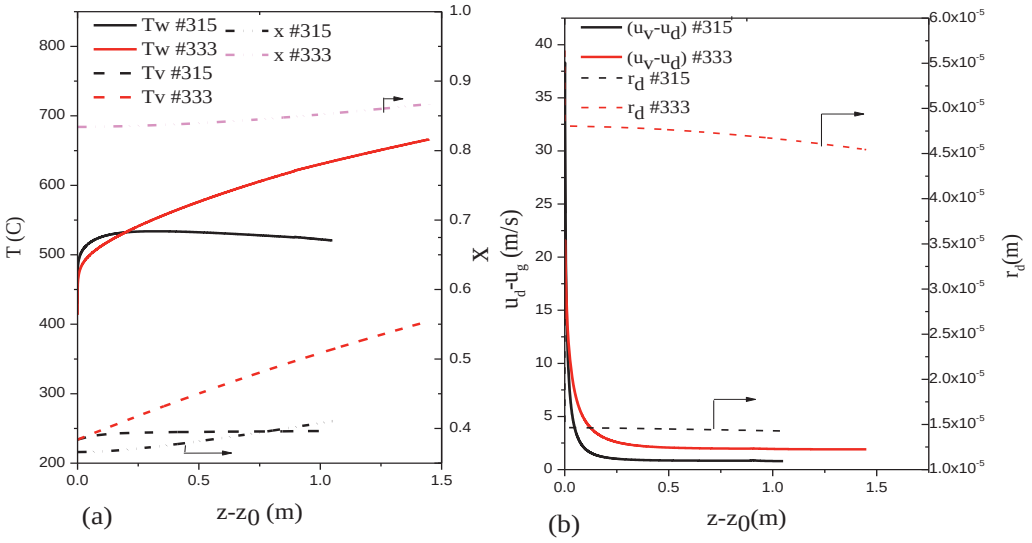

Figure 3. (a) wall temperature and vapor temperature change (b) relative velocity of droplets and radius change for the case #315 and #333 from Becker et al.[23]

#315: 30bar, G=1986.3 kg/m^{2}s , x_{do} = 0.366

#333: 30bar, G=496.9 kg/m^{2}s , x_{do} = 0.834

Figure 4 shows, under the same dryout quality and boiling number, the percentage of heat transfer rate from the vapor to the droplets for the cases of high and low degree of thermal non-equilibrium, respectively. For the case of low degree of thermal non-equilibrium, the heat transfer between vapor and droplets is significant; while the opposite cases show less amount of heat is transferred to the droplet, which reduce to the thermal non-equilibrium phenomenon. As for the pressure effect, the result indicates that the heat transfer between vapor and droplets is more effective at high pressures when it is under high

thermal non-equilibrium condition, and the evaporation of droplet will reduce the wall superheat. The calculated temperature, Figure 5, shows that the model successfully predicts the degree of thermal non-equilibrium and the trend of temperature change.

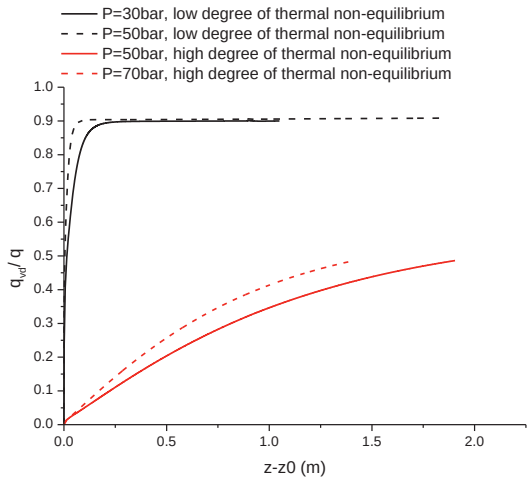

Figure 4. Heat transferred rate to the droplets in
(a) Cases of low degree of thermal non-equilibrium

$$\begin{cases}\text{\#315: 30bar, } x_{do}=0.366,\ G=1986.3\ \text{kg/m}^2\text{s},\ Bo=0.244\times10^{-3}\\ \text{\#282: 50bar, } x_{do}=0.316,\ G=3067.1\ \text{kg/m}^2\text{s},\ Bo=0.258\times10^{-3}\end{cases}$$ **from Becker et al.[23]**

(b) Cases of high degree of thermal non-equilibrium

$$\begin{cases}\text{\#307: 50bar, } x_{do}=0.876,\ G=498.1\ \text{kg/m}^2\text{s},\ Bo=0.686\times10^{-3}\\ \text{\#277: 70bar, } x_{do}=0.895,\ G=500.6\ \text{kg/m}^2\text{s},\ Bo=0.675\times10^{-3}\end{cases}$$ **from Becker et al.[23]**

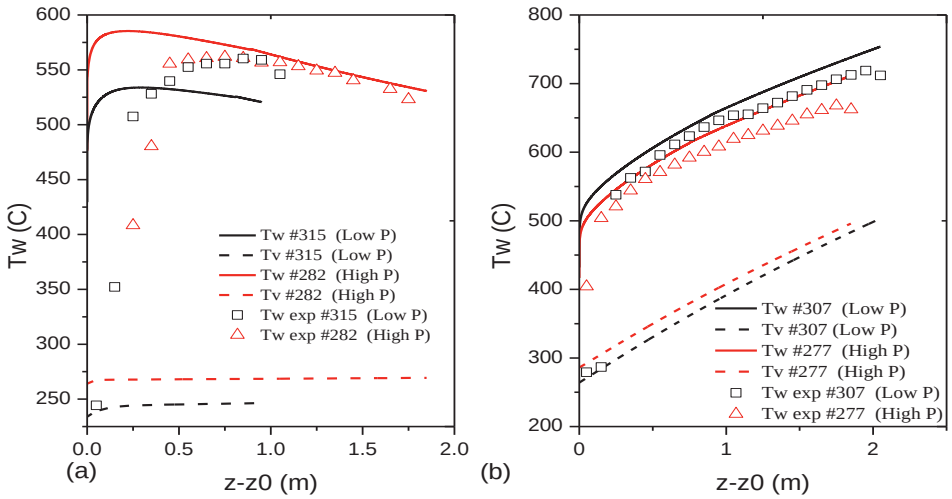

Figure 5. (a) Vapor and wall temperature prediction in low degree of thermal non-equilibrium

#315: 30bar, T_{sat} = 233.86 ^{o}C ,x_{do} =0.366, G=1986.3 kg/m^{2}s, Bo=0.244×10^{-3}

#282: 50bar, T_{sat} = 263.94 ^{o}C , x_{do} =0.316, G=3067.1 kg/m^{2}s, Bo=0.258×10^{-3} **from Becker et al.[23]**

(b) Vapor and wall temperature prediction in high degree of thermal non-equilibrium

#307: 50bar, T_{sat} = 263.94 ^{o}C , x_{do} =0.876, G=498.1 kg/m^{2}s, Bo=0.686×10^{-3}

#277: 70barT_{sat} = 285.83 ^{o}C, x_{do} =0.895, G=500.6 kg/m^{2}s, Bo=0.675×10^{-3} **from Becker et al.[23]**

Figure 6(a) shows the overall comparison of the wall temperature prediction with the experimental data. The predicted results show fairly good agreement with the experimental data. Over 90% of total 319 data can be predicted within $\pm 20\%$ from the present model. The discrepancy between the predicted T_w and experimental T_w are majorly for the data taken in the short distance beyond the dryout location. The reason may be attributed to the premature temperature rise in the prediction as indicated in Figure 5(a) and Figure 6(b). The present model does not consider the transition boiling from annular flow regime to post-dryout regime in which the liquid film and droplets may still have intense evaporation on the wall. As a consequence, this model can only be applied for the fully-developed post-dryout regime. As for the model being applied on the fully-developed post-dryout regime, the result shows a standard deviation of 6.3% and root-mean-square (RMS) error of 7.2%. More study considering transition region is under developing now.

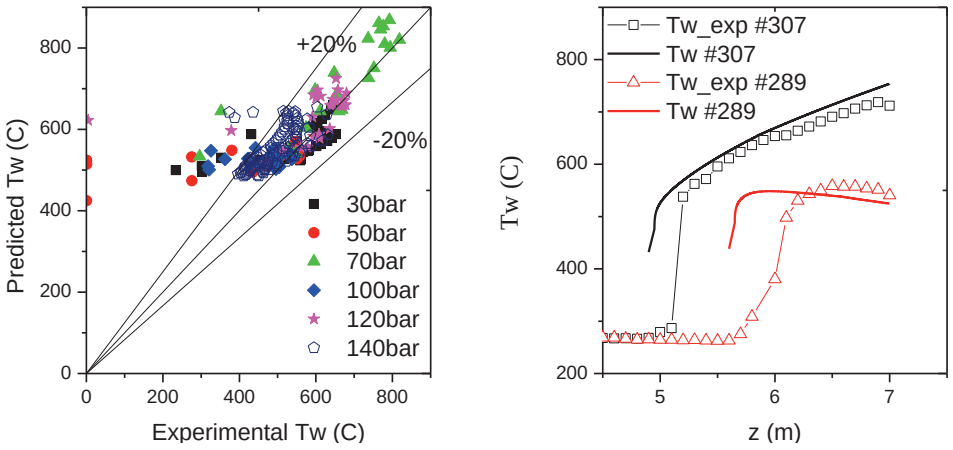

Figure 6. (a) Overall comparison of the predicted wall temperature with the experimental data. (b) The large discrepancy appears right beyond the dryout location.

5. SUMMARY AND CONCLUSION

A one-dimensional mechanistic model of fully-developed post-dryout heat transfer is proposed and evaluated in this paper. A correlation has been developed for the interfacial heat transfer between vapor and droplets, which modified the one by Ban and Kim[17] considering the contribution of Eckert number. This correlation indicates that in the post-dryout region, the viscous dissipation from droplet to vapor at the interface reduces the total heat transfer rate from vapor to droplets. Neglecting this phenomenon will lead to an overestimation of interfacial heat transfer rate.

319 experimental data points with the range of P= 30~140 bar, q"= 204~1837 kW/m^2 and G= 380~5180 kg/m^{2}s from Bennett et al.[27] and Becker et al.[23] are examined and compared with the present model predictions. The results show that the present model predicts fairly well in the wall temperature and the thermal non-equilibrium phenomenon in the fully-developed region, which give the standard deviation of 6.3% and RMS of 7.2%. The detail flowing information of vapor and droplets in the post-dryout region is also shown in the article. Comparing the difference between high and low degree of thermal non-equilibrium, the results show that the heat transferred to the droplets is significant in low degree of thermal non-equilibrium, but poor in another. As for the pressure effect, the heat transfer between vapor and droplets is more effective at high pressure when it is in high thermal non-equilibrium condition, and opposite is the case in low thermal non-equilibrium condition.

NOMENCLATURE

Bo	Boiling number $\frac{q''}{i_{lv}G}$
Cp	specific heat, kJ/ kgK
D	tube diameter, m
G	mass flux, kg/m^{2}s
g	gravitational constant, m/s^2
h	heat transfer coefficient, W/m^{2}K
i_{lv}	latent heat of evaporation, kJ/kg
k	thermal conductivity, W/mK
N	droplet flux, #/m^{2}s
Nu	Nusselt number $= \frac{hk}{D}$
Pr	Prandtl number = $\frac{Cp\mu}{k}$
q	heat flow rate, W
q''	heat flux, W/m^2
Re	Reynolds number = $\frac{\rho uD}{\mu}$
r	average radius
s	slip ratio
T	temperature, K
u	velocity, m/s
x	quality

Greek symbols

α	void fraction
μ	dynamic viscosity, Pa s
ρ	density, kg/m^3
σ	surface tension, N/m

Subscript

a	actual
c	critical
DO	dryout
d	droplet
f	film temperature

i	interfacial
l	saturation liquid
rwd	radiation between wall and droplets
rwv	radiation between wall and vapor
rvd	radiation between vapor and droplets
sd	single droplet
v	vapor
vd	vapor to droplet
w	wall
wd	wall to droplet
wv	wall to vapor

REFERENCES

1. R. S. Dougall and W. M. Rohsenow, "Film boiling on the inside of vertical tubes with upward flow of the fluid at low qualities," Cambridge, Mass.: Dept. of Mechanical Engineering, Massachusetts Institute of Technology,[1963]1963.
2. D. Groeneveld, "Post-dryout heat transfer: physical mechanisms and a survey of prediction methods," *Nuclear Engineering and Design,* **32**(3), pp. 283-294, (1975).
3. D. N. Plummer, "Post critical heat transfer to flowing liquid in a vertical tube," Cambridge, Mass.: Heat Transfer Laboratory, Department of Mechanical Engineering, Massachusetts Institute of Technology, 19741974.
4. D. Groeneveld and G. Delorme, "Prediction of thermal non-equilibrium in the post-dryout regime," *Nuclear Engineering and Design,* **36**(1), pp. 17-26, (1976).
5. P. Saha, "A nonequilibrium heat transfer model for dispersed droplet post-dryout regime," *International Journal of Heat and Mass Transfer,* **23**(4), pp. 483-492, (1980).
6. R. Forslund and W. M. Rohsenow, "Dispersed flow film boiling," *Journal of Heat Transfer,* **90**(4), pp. 399-407, (1968).
7. O. Iloeje, W. Rohsenow, and P. Griffith, "Three-Step Model of Dispersed Flow Heat Transfer (Post-CHF Vertical Flow)," *ASME Paper,* (1975).
8. E. Ganić and W. Rohsenow, "Dispersed flow heat transfer," *International Journal of Heat and Mass Transfer,* **20**(8), pp. 855-866, (1977).
9. R. A. Moose and E. Ganić, "On the calculation of wall temperatures in the post dryout heat transfer region," *International Journal of Multiphase Flow,* **8**(5), pp. 525-542, (1982).
10. Y. Guo and K. Mishima, "A non-equilibrium mechanistic heat transfer model for post-dryout dispersed flow regime," *Experimental thermal and fluid science,* **26**(6), pp. 861-869, (2002).
11. A. F. Varone and W. M. Rohsenow, "Post dryout heat transfer prediction," *Nuclear Engineering and Design,* **95**(pp. 315-327, (1986).
12. M. Andreani and G. Yadigaroglu, "Prediction methods for dispersed flow film boiling," *International Journal of Multiphase Flow,* **20**(pp. 1-51, (1994).
13. M. Andreani and G. Yadigaroglu, "A 3-D Eulerian-Lagrangian model of dispersed flow film boiling including a mechanistic description of the droplet spectrum evolution—I. The thermal-hydraulic model," *International Journal of Heat and Mass Transfer,* **40**(8), pp. 1753-1772, (1997).
14. M. J. Meholic, "The development of a non-equilibrium dispersed flow film boiling heat transfer modeling package," The Pennsylvania State University, 2011.

15. J. Heineman, "An experimental investigation of heat transfer to superheated steam in round and rectangular channels," Argonne National Lab., Ill.1960.
16. K. Lee and D. Ryley, "The evaporation of water droplets in superheated steam," *Journal of Heat Transfer*, **90**(4), pp. 445-451, (1968).
17. C. H. Ban and Y. Kim, "Evaporation of a water droplet in high-temperature steam," *Journal of the Korean Nuclear Society*, **32**(5), pp. 521-529, (2000).
18. H. D. Baehr and K. Stephan, *Heat and Mass Transfer*: Springer Berlin Heidelberg, 2006.
19. K. Sun, J. Gonzales-Santalo, and C. Tien, "Calculations of combined radiation and convection heat transfer in rod bundles under emergency cooling conditions," *Journal of Heat Transfer*, **98**(3), pp. 414-420, (1976).
20. M. Ishii and N. Zuber, "Drag coefficient and relative velocity in bubbly, droplet or particulate flows," *AIChE Journal*, **25**(5), pp. 843-855, (1979).
21. G. L. Yoder and W. M. Rohsenow, "A solution for dispersed flow heat transfer using equilibrium fluid conditions," *Journal of Heat Transfer*, **105**(1), pp. 10-17, (1983).
22. S. Ahmad, "Axial distribution of bulk temperature and void fraction in a heated channel with inlet subcooling," *Journal of Heat Transfer*, **92**(4), pp. 595-609, (1970).
23. K. M. Becker, *An Experimental Investigation of Post Dryout Heat Transfer*: Department of Nuclear Reactor Engineering, Royal Institute of Technology, 1983.
24. M. A. Woldesemayat and A. J. Ghajar, "Comparison of void fraction correlations for different flow patterns in horizontal and upward inclined pipes," *International Journal of Multiphase Flow*, **33**(4), pp. 347-370, (2007).
25. A. Cioncolini and J. R. Thome, "Void fraction prediction in annular two-phase flow," *International Journal of Multiphase Flow*, **43**(pp. 72-84, (2012).
26. I. Kataoka, M. Ishii, and K. Mishima, "Generation and size distribution of droplet in annular two-phase flow," *Journal of Fluids Engineering*, **105**(2), pp. 230-238, (1983).
27. A. Bennett, G. Hewitt, H. Kearsey, and R. Keeys, "Heat Transfer To steam-water mixtures flowing in uniformly heated tubes in which the critical heat flux has been exceeded," Atomic Energy Research Establishment, Harwell, Eng.1968.